Germline and Mosaic Variants in *PRKACA* and *PRKACB* Cause a Multiple Congenital Malformation Syndrome

Adrian Palencia-Campos,[1,2,27] Phillip C. Aoto,[3,27] Erik M.F. Machal,[4,27] Ana Rivera-Barahona,[1,2] Patricia Soto-Bielicka,[1] Daniela Bertinetti,[4] Blaine Baker,[3] Lily Vu,[3] Francesca Piceci-Sparascio,[5] Isabella Torrente,[5] Eveline Boudin,[6] Silke Peeters,[6] Wim Van Hul,[6] Celine Huber,[7,8] Dominique Bonneau,[9,10] Michael S. Hildebrand,[11,12] Matthew Coleman,[11,12] Melanie Bahlo,[13,14] Mark F. Bennett,[11,13,14] Amy L. Schneider,[11] Ingrid E. Scheffer,[11,12,15] Maria Kibæk,[16] Britta S. Kristiansen,[17] Mahmoud Y. Issa,[18] Mennat I. Mehrez,[19] Samira Ismail,[18] Jair Tenorio,[2,20,21] Gaoyang Li,[22] Bjørn Steen Skålhegg,[22] Ghada A. Otaify,[18] Samia Temtamy,[18] Mona Aglan,[18] Aia E. Jønch,[17] Alessandro De Luca,[5] Geert Mortier,[6,23] Valérie Cormier-Daire,[7,8] Alban Ziegler,[9,10] Mathew Wallis,[24,25] Pablo Lapunzina,[2,20,21] Friedrich W. Herberg,[4,28] Susan S. Taylor,[3,26,28] and Victor L. Ruiz-Perez[1,2,20,21,28,*]

Summary

PRKACA and *PRKACB* code for two catalytic subunits (Cα and Cβ) of cAMP-dependent protein kinase (PKA), a pleiotropic holoenzyme that regulates numerous fundamental biological processes such as metabolism, development, memory, and immune response. We report seven unrelated individuals presenting with a multiple congenital malformation syndrome in whom we identified heterozygous germline or mosaic missense variants in *PRKACA* or *PRKACB*. Three affected individuals were found with the same *PRKACA* variant, and the other four had different *PRKACB* mutations. In most cases, the mutations arose *de novo*, and two individuals had offspring with the same condition. Nearly all affected individuals and their affected offspring shared an atrioventricular septal defect or a common atrium along with postaxial polydactyly. Additional features included skeletal abnormalities and ectodermal defects of variable severity in five individuals, cognitive deficit in two individuals, and various unusual tumors in one individual. We investigated the structural and functional consequences of the variants identified in *PRKACA* and *PRKACB* through the use of several computational and experimental approaches, and we found that they lead to PKA holoenzymes which are more sensitive to activation by cAMP than are the wild-type proteins. Furthermore, expression of *PRKACA* or *PRKACB* variants detected in the affected individuals inhibited hedgehog signaling in NIH 3T3 fibroblasts, thereby providing an underlying mechanism for the developmental defects observed in these cases. Our findings highlight the importance of both Cα and Cβ subunits of PKA during human development.

Protein kinase A (PKA) can be found as an inactive tetrameric holoenzyme formed by the association of two catalytic (C) subunits with a regulatory (R) subunit dimer. Activation is achieved through binding of two molecules of cyclic AMP (cAMP) to each R-subunit and subsequent unleashing of the C-subunits to engage substrates. *PRKACA* (MIM: 601639) and *PRKACB* (MIM: 176892) code for the highly homologous Cα- and Cβ-subunits, respectively, and the four functionally non-redundant R-subunits (RIα, RIβ, RIIα, and RIIβ) are encoded by four genes (*PRKAR1A* [MIM: 188830], *PRKAR1B* [MIM: 176911], *PRKAR2A* [MIM: 176910], and *PRKAR2B* [MIM: 176912]).

[1]Instituto de Investigaciones Biomédicas "Alberto Sols," Consejo Superior de Investigaciones Científicas (CSIC)—Universidad Autónoma de Madrid (UAM), Madrid, 28029, Spain; [2]CIBER de Enfermedades Raras (CIBERER), Instituto de Salud Carlos III (ISCIII), Madrid, 28029, Spain; [3]Department of Pharmacology, University of California, San Diego, 9400 Gilman Drive, La Jolla, CA 92093-0654, USA; [4]Institute for Biology, Department of Biochemistry, University of Kassel, Kassel, 34132, Germany; [5]Medical Genetics Unit, Casa Sollievo della Sofferenza Foundation, IRCCS, San Giovanni Rotondo, 71013, Italy; [6]Department of Medical Genetics, University of Antwerp, Edegem, 2650, Belgium; [7]Clinical Genetics and Reference Center for Skeletal Dysplasia, AP-HP, Necker-Enfants Malades Hospital, Paris, 75015, France; [8]Université De Paris, INSERM UMR1163, Institut Imagine, Paris, 75015, France; [9]Biochemistry and Genetics Department, Angers Hospital, Angers Cedex 9, 49933, France; [10]UMR CNRS 6015—INSERM U1083, MitoVasc Institute, Angers University, Angers Cedex 9, 49933, France; [11]Epilepsy Research Centre, Department of Medicine, Austin Health, University of Melbourne, Heidelberg, 3084, Victoria, Australia; [12]Murdoch Children's Research Institute, Parkville, 3052, Victoria, Australia; [13]Population Health and Immunity Division, The Walter and Eliza Hall Institute of Medical Research, Parkville, 3052, Victoria, Australia; [14]Department of Medical Biology, University of Melbourne, Melbourne, 3010, Victoria, Australia; [15]Department of Paediatrics, University of Melbourne, Royal Children's Hospital, and Florey Institute of Neuroscience and Mental Health, Parkville, 3052, Victoria, Australia; [16]Children's Hospital of H.C. Andersen, Odense University Hospital, 5000 Odense, Denmark; [17]Department of Clinical Genetics, Odense University Hospital, 5000 Odense, Denmark; [18]Department of Clinical Genetics, Division of Human Genetics and Genome Research, Center of Excellence for Human Genetics, National Research Centre, Cairo, 12622, Egypt; [19]Department of Oro-dental Genetics, Division of Human Genetics and Genome Research. Center of Excellence for Human Genetics, National Research Centre, Cairo, 12622, Egypt; [20]Instituto de Genética Médica y Molecular (INGEMM)—IdiPAZ, Hospital Universitario La Paz, Universidad Autónoma, Madrid, 28046, Spain; [21]ITHACA, European Reference Network on Rare Congenital Malformations and Rare Intellectual Disability; [22]Division for Molecular Nutrition, Institute for Basic Medical Sciences, University of Oslo, Oslo, 0316, Norway; [23]Antwerp University Hospital, Edegem, 2650, Belgium; [24]School of Medicine and Menzies Institute for Medical Research, University of Tasmania, Hobart, Tasmania, 7001, Australia; [25]Clinical Genetics Service, Austin Health, Heidelberg, 3084, Victoria, Australia; [26]Department of Chemistry and Biochemistry, University of California, San Diego, 9400 Gilman Drive, La Jolla, CA 92093-0654, USA
[27]These authors contributed equally to this work
[28]These authors contributed equally to this work
*Correspondence: vlruiz@iib.uam.es
https://doi.org/10.1016/j.ajhg.2020.09.005.

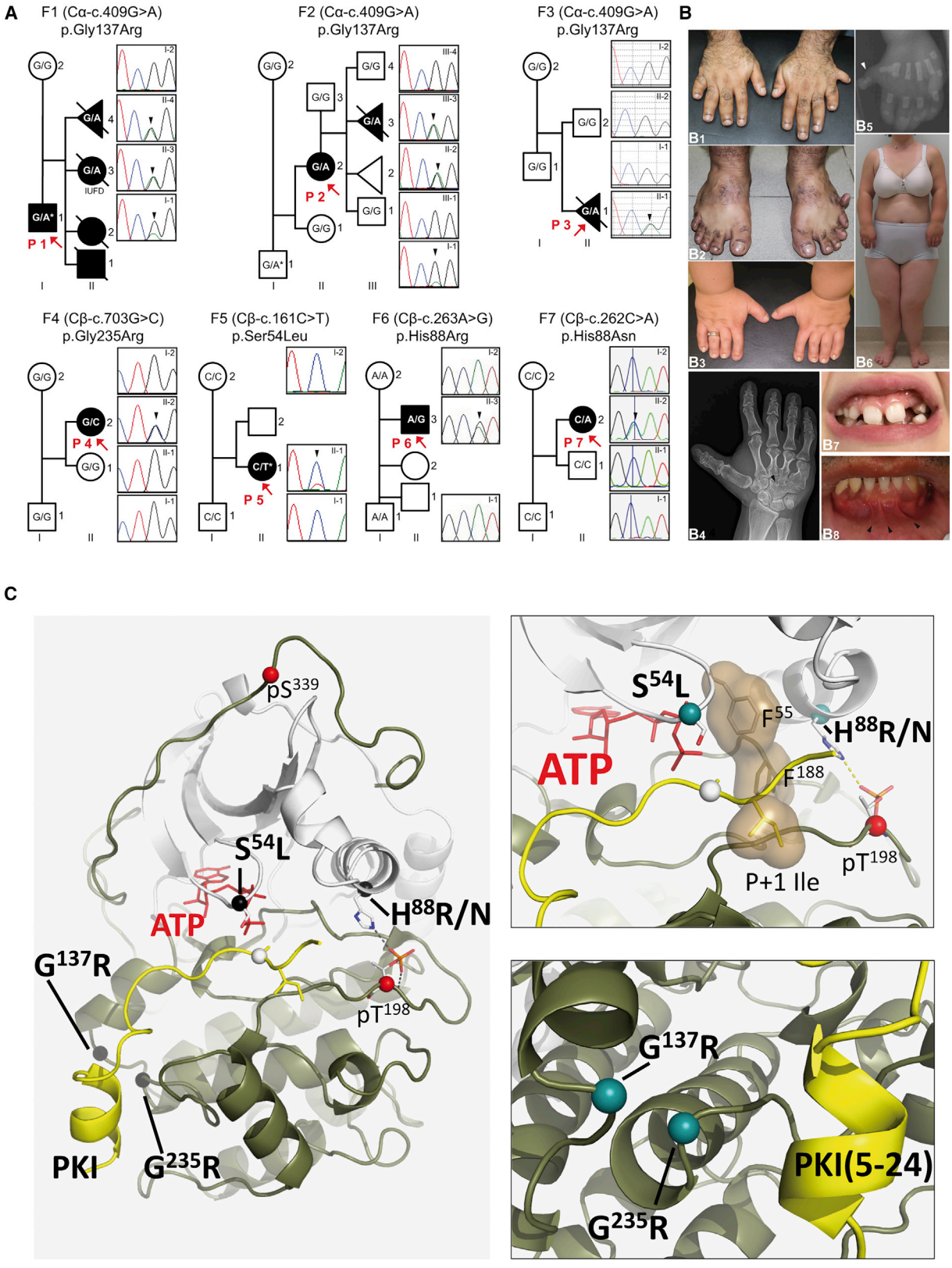

Figure 1. Affected Individuals and Mutations

(A) Family (F) pedigrees of the seven probands (P; red arrows) of this study and DNA sequence electropherograms illustrating mutations (black arrowheads) and their co-segregation with the disease phenotype. Asterisks denote mosaic state of the corresponding mutation in P1, the father of P2 (I-1) and in P5. IUFD: intrauterine fetal death.

(B) Clinical images. Hands and feet of P1 with bilateral postaxial polydactyly and wide sandal gap. The extra digit of the right hand and foot were surgically removed (B1 and B2). Hands of P2 demonstrating brachydactyly and nail dysplasia. Postaxial polydactyly had been

(legend continued on next page)

A-kinase anchoring proteins (AKAPs) and PKA inhibitor proteins (PKI) contribute to PKA subcellular localization and function by binding to R-subunits and C-subunits, respectively.[1]

PKA functions as an intracellular mediator of a variety of G-protein coupled receptor (GPCR) ligands, including specific hormones. Signaling from GPCRs coupled to protein Gαs stimulates adenylate cyclase, leading to increased levels of cAMP and consequently to higher PKA activity. The cAMP/PKA pathway is known to play a central role in the endocrine system because, in addition to mediating the effects of various hormones, it regulates hormone secretion and the proliferation of endocrine cells.[2]

In vertebrates, PKA also works to restrain hedgehog (Hh) signaling through phosphorylation of GLI transcription factors.[3,4] PKA-mediated phosphorylation of full-length GLI3 (GLI3-FL [MIM: 165240]) promotes the conversion of this factor into a strong transcriptional repressor (GLI3R) of Hh-target genes by inducing the proteolytic processing of its C-terminus. GLI3 has a dual function, and uncleaved GLI3FL can be transformed into a transcriptional activator (GLI3A). Hh ligands counteract the activity of PKA by de-repressing the main Hh signal transducer Smoothened (SMO [MIM: 601500]), which is classified as a Frizzled-class GPCR, and recruiting it into the primary cilium. Although the mechanism by which SMO regulates PKA is not fully elucidated, activated SMO suppresses PKA activity, at least partially, by removing from cilia the GPCR GPR161 [MIM: 612250], which presumably operates by increasing the levels of cAMP.[4–6]

PRKACA germline copy number gains have previously been associated with cortisol-producing bilateral adrenal hyperplasias and Cushing's syndrome (CS [MIM: 615830]),[7,8] and *PRKACA* somatic mutations are also found in tumors: cortisol-producing adrenal adenomas of CS individuals, hypothalamic hamartomas, and cardiac myxomas.[7,9,10] Similarly, a *PRKACB* somatic mutation was detected in tumor DNA from a CS individual,[11] and a 1p31.1 triplication encompassing *PRKACB* was described in another individual who had a specific form of Carney complex (CNC [MIM: 160980]) characterized by skin pigmentation, acromegaly, and myxomas, but not CS.[12]

Herein, we studied seven unrelated individuals of different ancestries (P1–P7; Figure 1A–B), all born to non-consanguineous healthy parents, who presented with congenital defects. Two individuals had offspring with the same condition, and the other five were simplex cases. All probands had limb abnormalities consisting of post-axial polydactyly of the hands (6/7 bilateral; 1/7 unilateral) and feet (4/7 bilateral; 1/7 unilateral) and brachydactyly (4/7). Congenital heart defects comprising common atrium or an atrioventricular septal defect (AVSD) were observed in 5/7 individuals. The two probands (P1, P2) without a heart condition had offspring with AVSD. Additionally, short stature/length, short limbs, narrow chest, abnormal teeth, oral frenula, nail dysplasia, and intellectual disability were features present in more than one affected individual. One proband had a history of unusual tumors. Affected individuals were initially diagnosed as having either Ellis-van Creveld syndrome (EvC; MIM: 225500), Weyers acrodental dysostosis (WAD; MIM: 193530), or an undiagnosed syndrome, depending on the presence and severity of chondroectodermal features (Table 1). Serum levels of hormones and bone metabolic markers were assessed in four affected individuals (P1, P2, P4, P7). Endocrine investigations did not show hypercortisolism or an overt endocrine dysfunction. Adrenal imaging in the same four probands (P1, P2, P4, P7) was also negative for adrenal abnormalities. An extended clinical description of the affected individuals is available as Supplemental Information (Supplemental Case Reports). The study was conducted in accordance with the declaration of Helsinki for medical research involving human subjects and was approved by the corresponding institutional ethics committees of the participant institutions. All affected individuals or their legal guardians and family members provided written informed consent for their participation in the study and publication of photographs.

After we excluded mutations in the EvC genes (*EVC* [MIM: 604831 and *EVC2* [MIM: 607261]), we conducted whole-exome sequencing (WES) in families 1 and 2. This analysis identified the same heterozygous missense variant in *PRKACA* (GenBank: NM_002730.4), c.409G>A (p.Gly137Arg), in both unrelated families. Remarkably, this mutation was also found in individual P3. The c.409G>A variant was mosaic in the unaffected father of P2 (variant allele fraction [VAF] = 0.16; altered allele read depth = 508/total read depth = 3,097), and was germline-transmitted in P2 (VAF = 0.55) and her affected offspring (VAF = 0.46). P1 was also mosaic for the same *PRKACA* variant (VAF = 0.28; 811/2,858), and his two affected offspring from whom there was available DNA (II-3 and II-4 in Figure 1A); both carried the variant in the heterozygous state. In P3, the mutation was identified as *de novo*. Next-generation sequencing (NGS) data for the c.409G>A variant and pedigree segregation were confirmed via Sanger sequencing in each family

previously corrected (B3). Radiograph of the right hand of P2 with carpal bone fusion (arrowhead) and brachydactyly (B4). Hand radiograph of III-3 (F2) showing postaxial polydactyly (arrowhead) (B5). Clinical image of P2 demonstrating short stature with short limbs (B6). Diastema and abnormal teeth in P4 at age 9 years (B7). Orodental features of P1 with diastema and multiple lower lingual frenula (arrowheads) (B8).

(C) Sites of mutations in the catalytic subunit of PKA. In the full-length C-subunit (left), the mutations are black spheres. p.Ser54Leu and p.His88Arg/Asn are near the active site (top right, teal spheres) and p.Gly137Arg and p.Gly235Arg (bottom right) are at a tethering surface that interacts with partner proteins, in this case the PKA inhibitor (PKI) peptide (yellow), whose tethering helix docks onto this site.

Table 1. Summary of Clinical and Molecular Findings of Affected Individuals

Clinical features (ethnic origin)	P1 (Egypt)	P2 (Belgium)	P3 (Italy)	P4 (Denmark)	P5 (France)	P6 (France)	P7 (Australia)
Age, gender	33 years, male	42 years, female	fetus (23 weeks), female	18 years, female	15 years, female	20 years, male	41 years, female
Height	165 cm (−1.61 SD)	139 cm (−5 SD); disproportionate short stature	fetus length: 27 cm (<3%)	163 cm (−1 SD)	148.5 cm (−1.8 SD)	175 cm (0 SD)	165 cm (−0.19 SD)
Weight	97 kg (+1.74 SD)	61,5 kg (+0.46 SD)	467 g (25% < p < 50%)	47.3 kg (−2.8 SD)	47 kg (−1 SD)	53 kg (−1.5 SD)	51.2 kg (−1.03 SD)
Head circumference	57 cm (+1.32 SD)	52,6 cm (−1.6 SD)	not available	51 cm (−3 SD)	55 cm (M)	56,5 cm (+ 0.5 SD)	56 cm (+ 1.18 SD)
Congenital heart abnormalities	no, but present in the affected offspring of the proband	no, but present in the affected offspring of the proband	yes, AVSD with myocardial hypertrophy	yes, AVSD and left cava superior entering into the coronary sinus	yes, single atrium, mitral anomaly	yes, single atrium, mild mitral valve regurgitation	yes, single atrium, surgically corrected in infancy; atrial fibrillation in adulthood with persistent incompetence of the valves
Postaxial polydactyly of the hands	yes, bilateral	yes, bilateral	yes, bilateral	yes, bilateral	yes, bilateral	yes, bilateral	yes, unilateral (right hand)
Postaxial polydactyly of the feet	yes, bilateral	no	yes, unilateral (hexadactyly of the left foot)	yes, bilateral	no	yes, bilateral	yes, bilateral
Other hands/ feet anomalies	brachydactyly	brachydactyly; fusion of hamate and capitate in right hand	not reported	short and broad with shortening of middle and distal phalanges and toes	brachydactyly and large great toe	fifth finger clinodactyly (unilateral)	fifth finger clinodactyly, broad toes, and mild digital clubbing
Long trunk	yes	yes, in childhood	not reported	yes	yes, moderate	no	no
Narrow thorax	no, but present in the affected offspring of the proband	yes, in childhood	yes, short ribs	yes	yes, moderate	no	no
Upper/ lower limb shortening	no (arm span 162 cm), but present in the affected offspring of the proband	yes (arm span 121 cm)	micromelia	yes	no	no	no
Genu valgum	yes	yes	not available	yes, genu valgum and previous surgery for coxa vara	yes	no	no, but recurrent dislocated patellae
Teeth abnormalities	yes, congenitally missing upper lateral incisors bilateral and lower right lateral incisor. Diastema	yes, conical teeth; early decay	not available	small central maxillary incisors, conical right canine, and hypodontia, invagination, agenesis, and supernumerary teeth of lateral mandibular incisors	yes, hypodontia	no	no
Nail dysplasia	no, but present in the affected offspring of the proband	yes	not available	yes, especially on the toes, also broad nails on both thumbs	no	no	no

(*Continued on next page*)

Table 1. ***Continued***

Clinical features (ethnic origin)	P1 (Egypt)	P2 (Belgium)	P3 (Italy)	P4 (Denmark)	P5 (France)	P6 (France)	P7 (Australia)
Facial/lip abnormalities	long face with mid face hypoplasia, short philtrum, overhanging nasal tip	notched upper lip	not available	long face, short and deep philtrum, tented upper lip	long face	no	broad forehead, hypertelorism, prognathism, prominent nasal tip
Multiple frenula or abnormal gum-lip attachment	yes, multiple upper and lower lingual frenula, hypoplastic maxilla with cross bite	multiple oral frenula at lower lip present at birth	not available	yes, abnormal gum-lip attachment	multiple oral frenula at lower lip	no	no
Intellectual disability	no	no	not applicable, fetus with brain edema	no, in childhood a period with mild developmental delay including mild language delay, gross motor difficulties, balance problems, and concentration problems; later diagnosed with dyslexia	no	yes, mild intellectual disability, reading and writing acquired, severe anxiety	yes, severe intellectual disability with autistic features. Medically refractory focal epilepsy
Neoplastic lesions	absent at age 33 years	absent at age 42 years	not reported	absent at age 18 years	absent at age 15 years	absent at age 20 years	yes, grade 1 borderline mucinous ovarian tumor, liver haemangioma, renal cell carcinoma
Clinical diagnosis	WAD	EvC	EvC	EvC	EvC	common atrium and polydactyly	common atrium and polydactyly
Affected gene variant description (GRCh37/hg19)	*PRKACA* chr19: 14211648 C>T NM_002730.4: c.409 G>A p.Gly137Arg	*PRKACA* chr19: 14211648 C>T NM_002730.4: c.409 G>A p.Gly137Arg	*PRKACA* chr19: 14211648 C>T NM_002730.4: c.409 G>A p.Gly137Arg	*PRKACB* chr1: 84668426 G>C NM_002731.3: c.703G>C p.Gly235Arg	*PRKACB* Chr1: 84647935 C>T NM_002731.3: c.161C>T p.Ser54Leu	*PRKACB* Chr1: 84649745 A>G NM_002731.3: c.263A>G p.His88Arg	*PRKACB* Chr1: 84649744 C>A NM_002731.3: c.262C>A p.His88Asn
Inheritance	mosaic	inherited	*de novo*	*de novo*	mosaic	*de novo*	*de novo*
NGS; altered allele reads/total read depth	0.28 (811/2,858)[a]	0.55 (41/74)	detected via Sanger sequencing; equal representation of altered and reference alleles in sequencing chromatograms	0.42 (102/239)	0.32 (39/122)	0.54 (20/37)	0.31 (4/13) (the mutant allele was demonstrated to be in the heterozygous state in blood-derived DNA of P7 [~59% mutant allele frequency] and absent in both parents via droplet digital PCR [ddPCR])

(*Continued on next page*)

Table 1. *Continued*

Clinical features (ethnic origin)	P1 (Egypt)	P2 (Belgium)	P3 (Italy)	P4 (Denmark)	P5 (France)	P6 (France)	P7 (Australia)
Other affected family members	yes, two offspring with postaxial polydactyly of both hands, short limbs, and congenital heart septal defects; both died early after birth; an IUFD at 33 weeks of gestation with bilateral postaxial polydactyly and congenital heart disease and a fetus with similar manifestations	yes, one affected fetus with short limbs, narrow thorax, postaxial polydactyly of both hands, and complete AVSD	no	no	no	no	no
Other information		surgery for a lobar emphysema in the left lung at the age of 2 years	the fetus presented with bicornuate and didelphys uterus; lungs with immature parenchyma at canalicular stage were also observed				dural ectasia and osteoporosis with multiple fractures

P: Proband. M: median or 50th percentile. AVSD: atrioventricular septal defect. WAD: Weyers acrodental dysostosis. EvC: Ellis-van Creveld syndrome. IUFD: Intrauterine fetal death. NGS: next-generation sequencing.
[a]To further confirm the mosaic state of the mutation detected by initial standard WES, additional deep WES was carried out in P1. Deep WES was also performed in the father of P2 (altered allele reads (508)/total read depth (3,097) = 0.16).

(Figure 1A, Table 1). Trio-WES in P4, P6, and P7 did not detect changes in *PRKACA* but revealed different *de novo* heterozygous missense variants predicted to be damaging in *PRKACB* (GenBank: NM_002731.3) in the three affected individuals (P4: c.703G>C [p.Gly235Arg], P6: c.263A>G [p.His88Arg], and P7: c.262C>A [p.His88Asn]). WES analysis of P5 also identified a pathogenic change in *PRKACB* (c.161C>T [p.Ser54Leu]). All four *PRKACB* variants were proved to be *de novo* through the use of Sanger sequencing. In P5, the mutation was present in 32% of NGS reads (VAF = 0.32; 39/122) and P5's electropherograms were consistent with this individual also being mosaic (Figure 1A, Table 1). All *PRKACA* and *PRKACB* variants were absent in gnomAD v2.1.1/v3[13] and involved evolutionarily conserved residues (Figure S1). Detailed WES results, including other variants detected and analysis pipelines used, are provided in the Supplemental Information (Figure S2). The p.Ser54Leu variant was previously identified as a somatic mutation in a cortisol-producing adenoma from an individual with CS.[11]

We next confirmed expression of Cα and Cβ transcripts in dermal fibroblasts through the use of RT-PCR (Figure S3A). Sequencing of the resulting RT-PCR fragments demonstrated expression of both normal and mutant *PRKACA* or *PRKACB* alleles in fibroblasts from affected individuals. We also observed the levels and localization of EvC proteins to be similar between cells from control and affected individuals (Figure S3B–S3C). Similarly, localization of PKA-C was found to be unaffected in *PRKACA*- or *PRKACB*-mutant fibroblasts (Figure S3D). In addition, because defects in one PKA subunit can lead to expression changes in other components of the holoenzyme,[14–16] we used qRT-PCR and immunoblotting to study PKA-C and -R expression in dermal fibroblasts. Compared to control cells, fibroblasts from individuals with *PRKACB* mutations showed a slight increase in the mRNA levels of *PRKACA*. PKA-C protein levels were also found to be increased in these cells, although statistical significance was only reached respecting one of the two controls included in the analysis. Furthermore, *PRKACB* mutant cells showed decreased *PRKAR1B* transcript levels. No significant differences, neither at the mRNA nor at the protein levels, of PKA-C or -R subunits were identified in fibroblasts from individuals with the *PRKACA* mutation with respect to controls. Changes in RIIβ protein levels were present in cells from both control and affected individuals and therefore cannot be attributed to the mutations (Figure S3E–S3F).

Analysis of the tertiary structure of the C-subunit revealed that mutations cluster in two groups with Cβ-Ser54 and Cβ-His88 being located in or near the Glycine-rich loop (G-Loop) at the active site and Cα-Gly137 and Cβ-Gly235 in a shared pocket at the end of the D and F helices (Figure 1C). Ensemble models, generated for each mutation, showed that both Cβ-p.His88Arg and Cβ-p.His88Asn altered the dynamics of the G-Loop, predictably affecting synergistic ATP and substrate peptide binding.[17,18] These

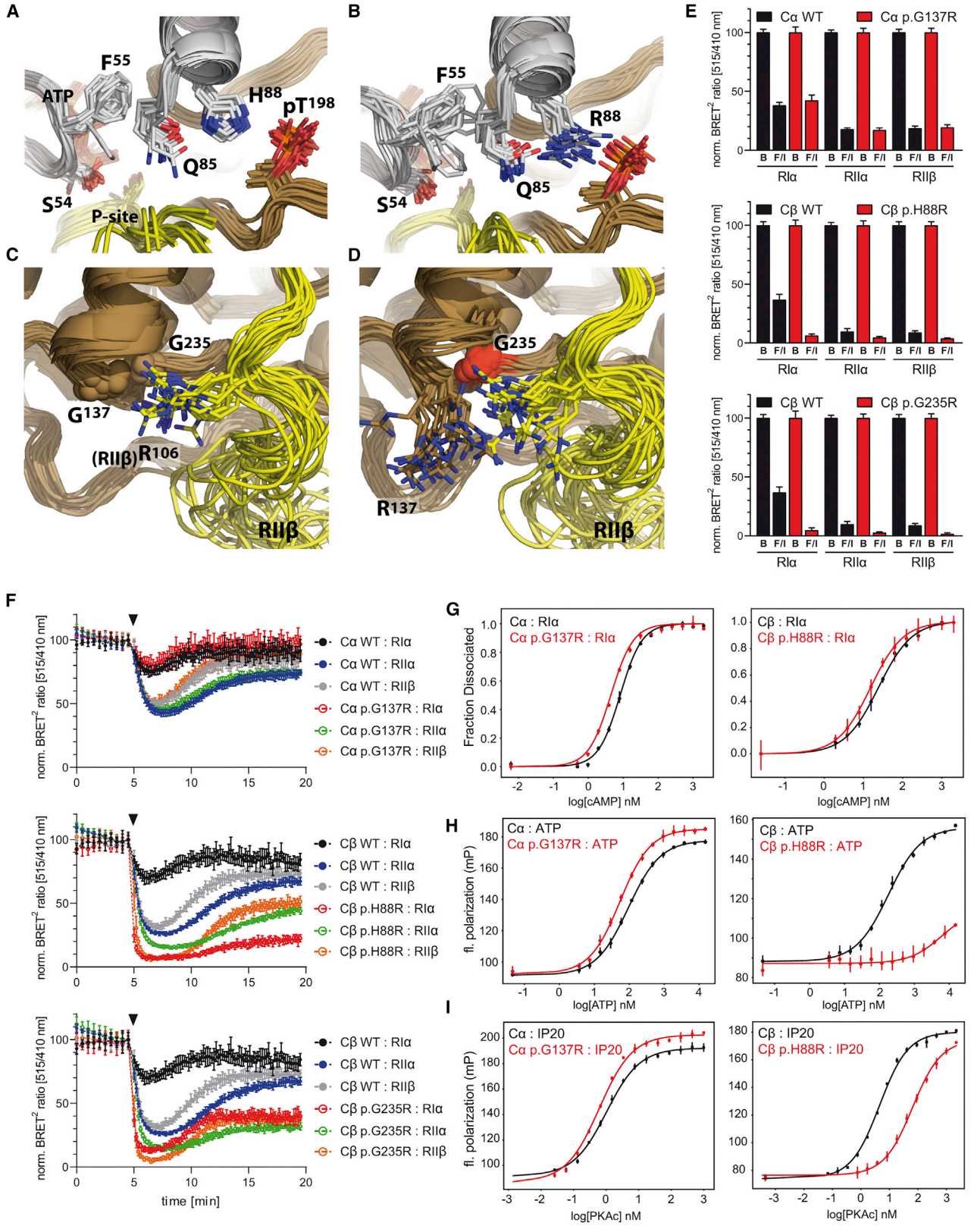

Figure 2. Structural and Functional Assessment of Mutations

(A–D.) Ensemble model of mutations: (A) A stabilizing four-residue network that involves salt bridges between the activation loop phosphate (phospho-Thr198), the C-helix (His88 and Gln85), and hydrophobic packing of Phe55 of the G-Loop onto Gln85 is found in WT PKA. This interaction modulates the conformational dynamics of the G-Loop.

(legend continued on next page)

mutations and the previously described Cβ-p.Ser54Leu[11] likely disrupt ATP-dependent regulation in the G-Loop. Cα-p.Gly137Arg and Cβ-p.Gly235Arg do not affect ATP binding, but they share an interface that forms interactions with regulatory proteins that include PKI, RIα, and RIIβ (Figure 2A–2D and Figure S4).

The effect of the identified mutations in PKA holoenzymes was analyzed by using bioluminescence resonance energy transfer ($BRET^2$), which provides *in cellulae* analysis of holoenzyme dissociation. This study showed a dramatic increase in the sensitivity to cAMP of Cβ-p.His88Arg and Cβ-p.Gly235Arg PKA holoenzymes formed with RIα, RIIα and RIIβ upon Forskolin/IBMX (Figure 2E) or isoproterenol (Figure 2F) stimulation in comparison to the corresponding Cβ-wild-type (Cβ-WT) PKA holoenzymes. Cβ-p.His88Asn showed almost full dissociation upon Forskolin/IBMX (Figure S5A) but a lower response to 100 nM isoproterenol compared to Cβ-p.His88Arg (Figure S5C and Figure 2F). Higher sensitivity to cAMP of the Cβ-p.His88Arg:RIα holoenzyme was additionally demonstrated through the use of fluorescence polarization assays (FPA). Using these assays, we also proved that the reduction in the stability of the Cβ-p.His88Arg:RIα holoenzyme can be attributed to loss of the synergistic effect of ATP binding, which is also true for the PKI peptide (PKI5-24) (Figure 2G–2I; Table S1). In contrast to the Cβ mutations, $BRET^2$ assays showed the dissociation kinetics for Cα-p.Gly137Arg and Cα-WT holoenzymes with RIα, RIIα, and RIIβ to be comparable (Figures 2E-2F). However, using FPA of purified holoenzymes (both RIα and RIIβ), we found greater sensitivity of Cα-p.Gly137Arg to lower cAMP concentration than the wild-type (WT) protein (Figure 2G and Figure S5D). Cα-p.Gly137Arg was additionally characterized with slightly increased cooperative binding for ATP and PKI peptide substrate (Figure 2H–2I; Table S1). Reduced association of Cα-p.Gly137Arg and Cβ-p.Gly235Arg with both RIα and RIIβ compared to their corresponding control C-WT proteins was also observed via co-immunoprecipitation (Figure S5E–S5F). Consistently, the kinase activity of Cα-p.Gly137Arg and Cβ-p.Gly235Arg determined through the use of the PepTag assay, which uses a fluorescent-labeled Kemptide substrate, in extracts from HEK293T co-transfected with both PKA-C and -RIα subunits, was found to be higher than that of their respective WT proteins at low cAMP concentrations (Figure S6).

Subsequently, we assessed the effect of mutations in the Hh pathway by ectopically expressing normal or mutant (Cα-p.Gly137Arg or Cβ-p.Gly235Arg) FLAG-tagged C-subunits together with RIα-GFP in NIH 3T3 via retroviral delivery. Notably, after stimulation of the pathway with the SMO-agonist SAG, the cells that were retrotransduced with the mutant C-subunits showed increased levels of GLI3R and reduced expression of the readout of the Hh pathway GLI1 compared to the control cultures, indicating that both Cα- and Cβ-mutations impair SAG-mediated inactivation of PKA in NIH 3T3 (Figure 3A–3D). Results were similar in cells treated only with FLAG-tagged C-subunit retroviruses (Figure S7). A model explaining the pathological mechanism of C-mutations in Hh signaling is shown in Figure 3E–3G.

In summary, we describe a syndrome involving multiple congenital anomalies caused by germline or mosaic mutations in *PRKACA* or *PRKACB*. Affected individuals had a constellation of features with the major shared findings being common atrium/AVSD and postaxial polydactyly. The association of these two features without other defects was postulated as an independent syndrome in a number of reported affected individuals.[24,25] Common atrium/AVSD and polydactyly are also part of the clinical spectrum of several ciliopathies, and their co-morbidity is often thought to be a consequence of abnormal Hh signaling.[26] Accordingly, germline or mosaic *PRKACA* or *PRKACB* mutations may explain the phenotype in other undiagnosed individuals with common atrium/AVSD-polydactyly alone or as part of more complex phenotypes.

Five of the seven probands in this report (P1–P5) showed phenotypic overlap with EvC or its less-severe dominantly inherited allelic form, WAD.[27] Biallelic loss-of-function

(B) The p.His88Arg (R88) mutation pulls Gln85 away from Phe55 and releases the G-Loop, likely leading to reduced synergistic binding of ATP and reduced affinity for the ATP-dependent RIα subunit. p.Ser54Leu, in the G-Loop, likely similarly affects ATP-dependent regulation by disrupting the G-Loop dynamics.
(C) In WT PKA, a pocket is formed by the D and F helices, and that pocket is accessed in an RIIβ-specific manner by Arg106 in the inhibitor segment (PDB:3TNP) and by the tethering helix in PKI(5-24).
(D) p.Gly137Arg and p.Gly235Arg disturb this RIIβ-specific interaction. This pocket is also at the RIα cAMP-binding domain-B interface (PDB:6NO7) and at the interface with the tethering helix in PKI (Figure S4B–S4C).
(E) In $BRET^2$ experiments, Cα-p.Gly137Arg shows comparable dissociation to that of Cα-WT upon full cAMP-stimulation by Forskolin/IBMX (F/I) for RIα-, RIIα, and RIIβ-holoenzymes, whereas Cβ-p.His88Arg- and Cβ-p.Gly235Arg-holoenzymes fully dissociate. $BRET^2$ data from unstimulated cells treated with buffer only are designated by the letter B. Normalized data are shown as means ± SD of three independent experiments with n = 6 replicates each (total n = 18).
(F) Kinetic $BRET^2$ analyses demonstrate full dissociation upon addition of the physiological β-adrenergic agonist isoproterenol (100 nM, triangle) for Cβ-p.His88Arg and Cβ-p.Gly235Arg and identical behavior of Cα-WT and Cα-p.Gly137Arg. Data shown are means ± SD of n = 6 replicates showing one of three (two for RIIα) independent experiments. For expression levels of GFP-C-subunits used in BRET, see Figure S5B.
(G) FPA analysis: RIα holoenzyme activation by cAMP shows increased sensitivity compared to WT with both Cα-p.Gly137Arg and Cβ-p.His88Arg (n = 3).
(H–I) FPA: Synergistic binding of ATP (H) with PKI 5-24 (IP20) peptide (I) to the C-subunit shows slightly increased binding affinity compared to WT with Cα-p.Gly137Arg and strongly decreased cooperativity with Cβ-p.His88Arg (n = 3). To illustrate differences in total binding, raw fluorescence polarization is expressed as millipolarization units (mP), and otherwise mP has been converted to fraction dissociated. Graphs show the mean ± SD.

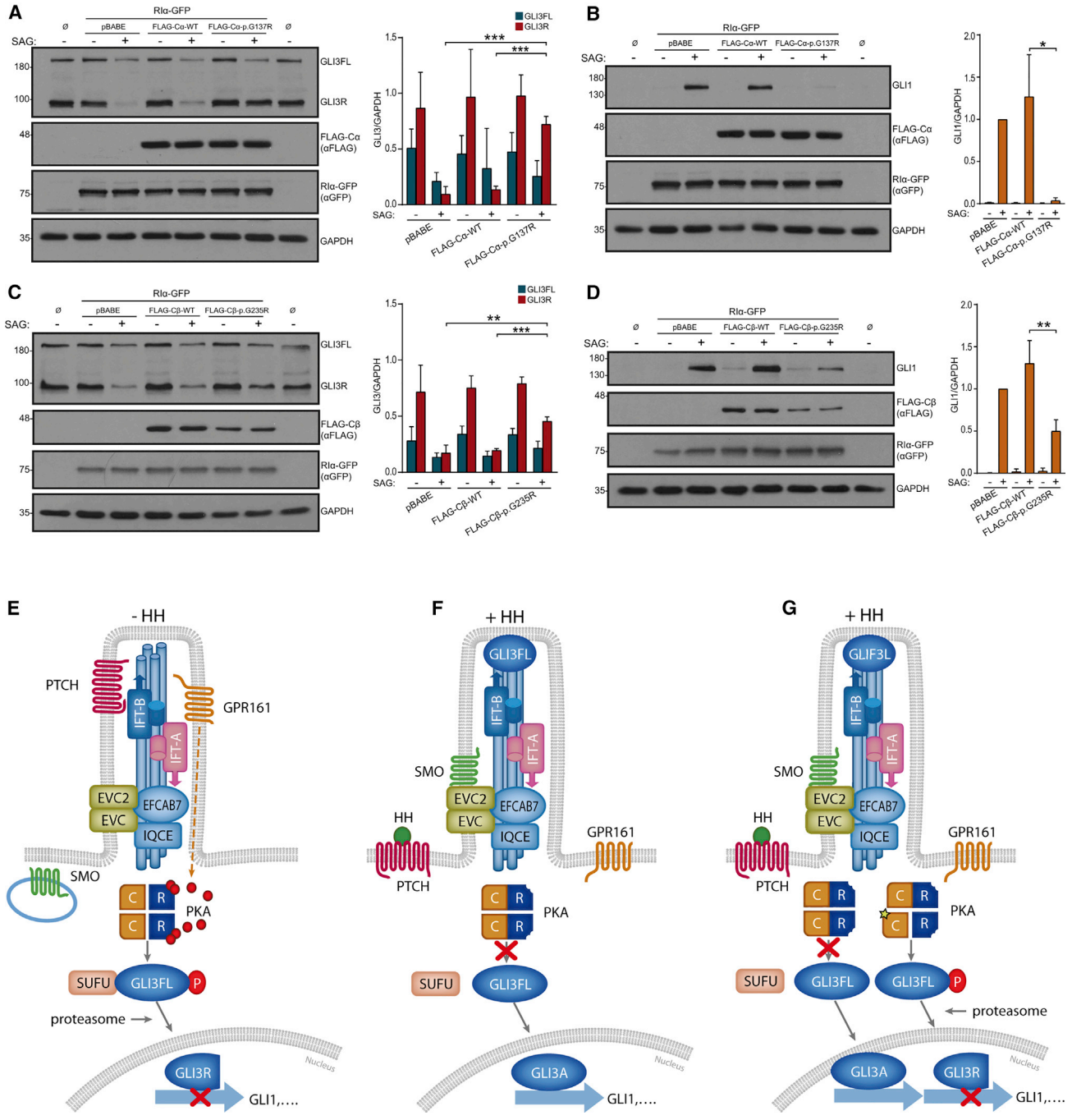

Figure 3. ***PRKACA* and *PRKACB* Mutations Impair Hh Signaling in NIH 3T3**

(A–D) Analysis of GLI3 and GLI1 protein levels in NIH 3T3 co-infected with human FLAG-Cα-WT or FLAG-Cα-p.Gly137Arg and RIα-GFP retroviral vectors (A–B) or alternatively with FLAG-Cβ-WT or FLAG-Cβ-p.Gly235Arg and RIα-GFP retroviruses (C–D), exposed to SAG (+) or its vehicle DMSO (-). Non-infected cells are indicated with Ø. Expression levels of FLAG-C and RIα-GFP are shown in the underneath panels. After incubation with SAG, Cα-p.Gly137Arg and Cβ-p.Gly235Arg retrotransduced cells showed increased GLI3R protein levels and reduced expression of GLI1 compared to cells retrotransduced with pBABE (empty vector) or with FLAG-Cα-WT or FLAG-Cβ-WT. Representative immunoblots are on the left and histograms show densitometric quantification of the levels of GLI3R and GLI3FL referred to GAPDH in (A) and (C), or GLI1/GAPDH levels normalized to the value of SAG-pBABE cells in (B) and (D). Data are expressed as mean ± SD from three experiments corresponding to three independent retroviral infections (n = 3). * = $p < 0.05$; ** = $p < 0.01$; *** = $p < 0.001$. Student's t-test.

(E–G) Model of action of PKA-Cα/β mutations. (E) In the absence of signal, PTCH (the receptor of Hh ligands [HH]) is in the cilium and represses SMO. GPR161 is also located in the cilium membrane and negatively regulates Hh signaling by promoting adenylyl-cyclase-dependent cAMP synthesis (red spheres). Consequently, PKA holoenzymes are active and their C-subunits (C) are free from R-subunits (R) to phosphorylate GLI3FL, which is bound to the inhibitory protein SUFU. Phosphorylated GLI3FL undergoes C-terminal proteolytic processing by the proteasome and is transformed into GLI3R, leading to reduced expression of Hh targets such as GLI1. (F) The

(legend continued on next page)

mutations in *EVC* or *EVC2*, which encode the two subunits of the EvC ciliary complex (EVC and EVC2), are the primary cause of EvC, whereas specific heterozygous C-terminal truncating mutations in *EVC2* are responsible for WAD.[28–30] The EvC complex, which localizes at the base of primary cilia, is required downstream of SMO for complete inhibition of GLI3FL processing in response to Hh ligands.[20–22] Consequently, PKA and EVC-EVC2 act at the same level in the Hh pathway, but in an opposing manner. A scaffolding role for concentrating SMO signaling to the cilium base has been proposed for the EVC-EVC2 complex.[4,21] Given the overlap between EvC/WAD and *PRKACA/B* phenotypes, EVC-EVC2 could specifically link SMO signaling to PKA acting as scaffold, or be involved in a biochemical reaction to prevent the phosphorylation of GLI3 by PKA. Intriguingly, RIα is known to bind specifically to GPR161.[31] The ciliopathy-like phenotype of the individuals of this report is in agreement with the negative effect caused by the identified *PRKACA* and *PRKACB* variants on Hh signaling. However, we cannot rule out the possibility that these mutations could also alter additional molecular pathways regulated by PKA that may be contributing to the phenotype. Skeletal defects have been reported in association with variants in other PKA subunits or other components of cAMP/PKA signaling. Specific variants in *PRKAR1A* lead to acrodysosotosis type 1 (MIM: 101800),[32] and variants in the cAMP phosphodiesterase encoded by *PDE4D* lead to acrodysostosis type 2 (MIM 614613).[33,34] The skeletal phenotype of acrodysostosis (brachydactyly, short stature, facial dysostosis, and nasal hypoplasia) is similar to that of Albright hereditary osteodystrophy and does not typically resemble a ciliopathy. Loss-of-function mutations in *PRKAR1A* resulting in unrestricted PKA activity cause CNC,[35] which is a condition characterized by skin pigmentary abnormalities, endocrine tumors or overactivity, and other tumors such as myxomas or schwannomas. However, polydactyly, common atrium/AVSD, and skeletal and ectodermal defects are not considered to be part of the CNC diagnostic criteria.[36] *Prkar1a*$^{+/-}$ mice have also been shown to be prone to developing bone lesions.[14,15] Considering the individuals reported here, only P7 had tumors, but she did not have evidence of CS, and to date, no adrenal, pituitary, or thyroid tumors have been found on imaging. She did not have the typical skin manifestations of CNC, either. Whether the presence of tumors in P7 is due to the Cβ-p.His88Asn variant needs to be clarified through further investigations. The hormonal profile in the four affected individuals analyzed did not show signs of overt endocrine alterations, and until now, bone tumors have not been identified in any of the affected individuals.

We show that the mutations reported here affect the interaction of C- and R-subunits through an ATP-dependent mechanism (for p.His88Arg, p.His88Asn, and p.Ser54Leu) or through disruption of interfacial surfaces (for p.Gly137Arg and p.Gly235Arg), creating holoenzymes that are more sensitive to cAMP for different reasons. This implies that the mutant Cα- and Cβ-subunits remain more active following the downregulation of cAMP levels associated with Hh signaling,[23] thus decreasing the strength of this pathway. Indeed, diminished Hh signaling activity was observed in NIH 3T3 ectopically expressing mutant C-subunits. Of note, using random mutagenesis in a plasmid containing the mouse Cα subunit, Orellana and McKnight described a p.His87Gln variant (p.His88Gln using our variant nomenclature) that compared to the WT protein retained partial activity in the presence of an excess of RIα subunit.[37]

In our assays, Cα-p.Gly137Arg caused a less severe impact in PKA holoenzymes than the Cβ mutations did. Because Cα is the major PKA C-subunit and is ubiquitously expressed, whereas Cβ is mainly expressed in brain and lymphoid tissues,[38] mutations in Cβ may need to be more damaging than in Cα in order to cause a phenotype in tissues with low Cβ expression. Nonetheless, we cannot discard the possibility that Cα-p.Gly137Arg could also alter an unknown Hh-specific regulatory mechanism of PKA inactivation. During the preparation of this manuscript, we became aware of a large-scale clinical exome sequencing study compiling WES results from >2,200 Saudi families; in this study, the Cα-p.Gly137Arg variant was observed to be *de novo* in one affected individual with clinical suspicion of EvC. The WES result of this individual was stated as ambiguous, and the case was considered not solved because of the unknown causality of the change, which is now demonstrated by our data.[39] This observation further reinforces the recurrent character of the Cα-p.Gly137Arg mutation. While much is known about the Cα-subunit, surprisingly little is known about the Cβ-subunit. Our discovery of these mutations underscores the need to now distinguish between the structural and functional differences of Cβ splice variants that remain as an

interaction of Hh ligands with PTCH disables this protein to continue repressing SMO and PTCH-HH complexes exit from cilia. Derepressed SMO accumulates into the cilium and interacts with the EvC ciliary complex, which is retained at the base of this organelle through binding of the C-terminal of EVC2 to the EFCAB7-IQCE complex.[19] In this manner, SMO signaling is enriched at the EvC region. SMO and the EvC proteins promote GLI3FL-SUFU dissociation and stimulate the recruitment of GLI3 to cilia tips.[20–22] Active SMO additionally causes GPR161 to abandon the cilium, and this, in combination with other not fully understood SMO-mediated mechanisms, results in decreased levels of cAMP and the inactivation of PKA.[4,23] Accordingly, GLI3FL phosphorylation is stopped and the production of GLI3R discontinued while GLI3FL is converted into a functional transcriptional activator (GLI3A). (G) The same situation as in (F), but in an individual with a *PRKACA* or *PRKACB* mutation. Due to higher cAMP sensitivity of the mutant PKA holoenzymes, the mutant PKA C-subunits (star) remain active following downregulation of cAMP levels associated with the activation of the Hh pathway, thus leading to abnormally increased levels of GLI3R and reduced Hh pathway activity. Affected individuals are expected to have holoenzymes containing two normal or two mutant C-subunits and holoenzymes composed of one normal and one mutant C-subunit. Intraflagellar transport protein complexes (IFT-A and IFT-B) which are also involved in Hh signaling are indicated in (E–G).

unexplored frontier. Our findings demonstrate a critical role of both Cα- and Cβ-subunits of PKA in human development.

Data and Code Availability

Specific datasets supporting this article or additional information not subjected to ethical restrictions can be obtained from the corresponding author upon request.

Supplemental Data

Supplemental Data can be found online at https://doi.org/10.1016/j.ajhg.2020.09.005.

Acknowledgments

We thank all affected individuals, their siblings, and their parents or legal guardians for their participation in this study. Some individuals were included after a GeneMatcher match.[40] This work was partially supported by funding from the Spanish Ministry of Science, Innovation and Universities (SAF2016-75434-R [AEI/FEDER, UE] and PID2019-105620RB-I00/AEI/10.13039/501100011033) to V.L.R.-P. S.S.T. was supported by NIH grant R03TR002947, E.M.F.M. by Kassel graduate school "Clocks", and A.D.L. by the Italian Ministry of Health (RC-2019). The University of Antwerp supported G.M. and W.V.H. with Methusalem funding (FFB190208) and S.P. with a predoctoral grant. E.B. was supported by The Research Foundation Flanders with a postdoctoral grant (12A3814N). The study was also funded by a National Health and Medical Research Council Program Grant (1091593) to I.E.S., a Practitioner Fellowship (1006110) to I.E.S., a Senior Research Fellowship (1102971) to M.B., and an R.D. Wright Career Development Fellowship (1063799) to M.S.H. B.S.S. and G.L. were supported by Throne Holst Foundation UiO (2019-2021) and Strategic PhD fund by UiO/IMB.

Declaration of Interests

I.E.S has served on scientific advisory boards for UCB, Eisai, GlaxoSmithKline, BioMarin, Nutricia, and Xenon Pharmaceuticals and on editorial boards of the Annals of Neurology, Neurology and Epileptic Disorders; may accrue future revenue on pending patent WO61/010176 (filed: 2008): Therapeutic Compound, a patent for SCN1A testing held by Bionomics Inc. and licensed to various diagnostic companies; has received speaker honoraria from GlaxoSmithKline, Athena Diagnostics, UCB, BioMarin, Biocodex, Eisai, and Transgenomics; and has received funding for travel from Athena Diagnostics, UCB, Biocodex, GlaxoSmithKline, Biomarin, and Eisai. The remaining authors declare no competing interests.

Received: April 28, 2020
Accepted: September 9, 2020
Published: October 14, 2020

Web Resources

ClinVar, https://www.ncbi.nlm.nih.gov/clinvar/
dbSNP, https://www.ncbi.nlm.nih.gov/snp/
gnomAD Browser, https://gnomad.broadinstitute.org/
OMIM, https://www.omim.org/
UCSC Genome Browser, https://genome.ucsc.edu/

References

1. Søberg, K., and Skålhegg, B.S. (2018). The Molecular Basis for Specificity at the Level of the Protein Kinase a Catalytic Subunit. Front. Endocrinol. (Lausanne) *9*, 538.
2. Peverelli, E., Mantovani, G., Lania, A.G., and Spada, A. (2013). cAMP in the pituitary: an old messenger for multiple signals. J. Mol. Endocrinol. *52*, R67–R77.
3. Huang, Y., Roelink, H., and McKnight, G.S. (2002). Protein kinase A deficiency causes axially localized neural tube defects in mice. J. Biol. Chem. *277*, 19889–19896.
4. Kong, J.H., Siebold, C., and Rohatgi, R. (2019). Biochemical mechanisms of vertebrate hedgehog signaling. Development *146*, dev166892. https://doi.org/10.1242/dev.166892.
5. Mukhopadhyay, S., Wen, X., Ratti, N., Loktev, A., Rangell, L., Scales, S.J., and Jackson, P.K. (2013). The ciliary G-protein-coupled receptor Gpr161 negatively regulates the Sonic hedgehog pathway via cAMP signaling. Cell *152*, 210–223.
6. Nachury, M.V., and Mick, D.U. (2019). Establishing and regulating the composition of cilia for signal transduction. Nat. Rev. Mol. Cell Biol. *20*, 389–405.
7. Beuschlein, F., Fassnacht, M., Assié, G., Calebiro, D., Stratakis, C.A., Osswald, A., Ronchi, C.L., Wieland, T., Sbiera, S., Faucz, F.R., et al. (2014). Constitutive activation of PKA catalytic subunit in adrenal Cushing's syndrome. N. Engl. J. Med. *370*, 1019–1028.
8. Carney, J.A., Lyssikatos, C., Lodish, M.B., and Stratakis, C.A. (2015). Germline PRKACA amplification leads to Cushing syndrome caused by 3 adrenocortical pathologic phenotypes. Hum. Pathol. *46*, 40–49.
9. Hildebrand, M.S., Griffin, N.G., Damiano, J.A., Cops, E.J., Burgess, R., Ozturk, E., Jones, N.C., Leventer, R.J., Freeman, J.L., Harvey, A.S., et al. (2016). Mutations of the Sonic Hedgehog Pathway Underlie Hypothalamic Hamartoma with Gelastic Epilepsy. Am. J. Hum. Genet. *99*, 423–429.
10. Tseng, I.C., Huang, W.J., Jhuang, Y.L., Chang, Y.Y., Hsu, H.P., and Jeng, Y.M. (2017). Microinsertions in PRKACA cause activation of the protein kinase A pathway in cardiac myxoma. J. Pathol. *242*, 134–139.
11. Espiard, S., Knape, M.J., Bathon, K., Assié, G., Rizk-Rabin, M., Faillot, S., Luscap-Rondof, W., Abid, D., Guignat, L., Calebiro, D., et al. (2018). Activating PRKACB somatic mutation in cortisol-producing adenomas. JCI Insight *3*, e98296. https://doi.org/10.1172/jci.insight.98296.
12. Forlino, A., Vetro, A., Garavelli, L., Ciccone, R., London, E., Stratakis, C.A., and Zuffardi, O. (2014). PRKACB and Carney complex. N. Engl. J. Med. *370*, 1065–1067.
13. Karczewski, K.J.J., Francioli, L.C., Tiao, G., Cummings, B.B., Alföldi, J., Wang, Q., Collins, R.L., Laricchia, K.M., Ganna, A., Birnbaum, D.P., et al. (2019). Variation across 141,456 human exomes and genomes reveals the spectrum of loss-of-function intolerance across human protein-coding genes. bioRxiv. https://doi.org/10.1101/531210.
14. Liu, S., Saloustros, E., Mertz, E.L., Tsang, K., Starost, M.F., Salpea, P., Faucz, F.R., Szarek, E., Nesterova, M., Leikin, S., and Stratakis, C.A. (2015). Haploinsufficiency for either one of the type-II regulatory subunits of protein kinase A improves the bone phenotype of Prkar1a+/- mice. Hum. Mol. Genet. *24*, 6080–6092.
15. Tsang, K.M., Starost, M.F., Nesterova, M., Boikos, S.A., Watkins, T., Almeida, M.Q., Harran, M., Li, A., Collins, M.T., Cheadle, C., et al. (2010). Alternate protein kinase A activity

identifies a unique population of stromal cells in adult bone. Proc. Natl. Acad. Sci. USA *107*, 8683–8688.
16. Yin, Z., Pringle, D.R., Jones, G.N., Kelly, K.M., and Kirschner, L.S. (2011). Differential role of PKA catalytic subunits in mediating phenotypes caused by knockout of the Carney complex gene Prkar1a. Mol. Endocrinol. *25*, 1786–1793.
17. Taylor, S.S., Yang, J., Wu, J., Haste, N.M., Radzio-Andzelm, E., and Anand, G. (2004). PKA: a portrait of protein kinase dynamics. Biochim. Biophys. Acta *1697*, 259–269.
18. Lew, J., Coruh, N., Tsigelny, I., Garrod, S., and Taylor, S.S. (1997). Synergistic binding of nucleotides and inhibitors to cAMP-dependent protein kinase examined by acrylodan fluorescence spectroscopy. J. Biol. Chem. *272*, 1507–1513.
19. Pusapati, G.V., Hughes, C.E., Dorn, K.V., Zhang, D., Sugianto, P., Aravind, L., and Rohatgi, R. (2014). EFCAB7 and IQCE regulate hedgehog signaling by tethering the EVC-EVC2 complex to the base of primary cilia. Dev. Cell *28*, 483–496.
20. Caparrós-Martín, J.A., Valencia, M., Reytor, E., Pacheco, M., Fernandez, M., Perez-Aytes, A., Gean, E., Lapunzina, P., Peters, H., Goodship, J.A., and Ruiz-Perez, V.L. (2013). The ciliary Evc/Evc2 complex interacts with Smo and controls Hedgehog pathway activity in chondrocytes by regulating Sufu/Gli3 dissociation and Gli3 trafficking in primary cilia. Hum. Mol. Genet. *22*, 124–139.
21. Dorn, K.V., Hughes, C.E., and Rohatgi, R. (2012). A Smoothened-Evc2 complex transduces the Hedgehog signal at primary cilia. Dev. Cell *23*, 823–835.
22. Yang, C., Chen, W., Chen, Y., and Jiang, J. (2012). Smoothened transduces Hedgehog signal by forming a complex with Evc/Evc2. Cell Res. *22*, 1593–1604.
23. Moore, B.S., Stepanchick, A.N., Tewson, P.H., Hartle, C.M., Zhang, J., Quinn, A.M., Hughes, T.E., and Mirshahi, T. (2016). Cilia have high cAMP levels that are inhibited by Sonic Hedgehog-regulated calcium dynamics. Proc. Natl. Acad. Sci. USA *113*, 13069–13074.
24. Levin, S.E., Dansky, R., Milner, S., Benatar, A., Govendrageloo, K., and du Plessis, J. (1995). Atrioventricular septal defect and type A postaxial polydactyly without other major associated anomalies: a specific association. Pediatr. Cardiol. *16*, 242–246.
25. Onat, T. (1994). Post-axial hexodactily and single atrium: a new syndrome? Hum. Genet. *94*, 104–106.
26. Digilio, M.C., Pugnaloni, F., De Luca, A., Calcagni, G., Baban, A., Dentici, M.L., Versacci, P., Dallapiccola, B., Tartaglia, M., and Marino, B. (2019). Atrioventricular canal defect and genetic syndromes: The unifying role of sonic hedgehog. Clin. Genet. *95*, 268–276.
27. Ruiz-Perez, V.L., and Goodship, J.A. (2009). Ellis-van Creveld syndrome and Weyers acrodental dysostosis are caused by cilia-mediated diminished response to hedgehog ligands. Am. J. Med. Genet. C. Semin. Med. Genet. *151C*, 341–351.
28. Ruiz-Perez, V.L., Ide, S.E., Strom, T.M., Lorenz, B., Wilson, D., Woods, K., King, L., Francomano, C., Freisinger, P., Spranger, S., et al. (2000). Mutations in a new gene in Ellis-van Creveld syndrome and Weyers acrodental dysostosis. Nat. Genet. *24*, 283–286.
29. Ruiz-Perez, V.L., Tompson, S.W., Blair, H.J., Espinoza-Valdez, C., Lapunzina, P., Silva, E.O., Hamel, B., Gibbs, J.L., Young, I.D., Wright, M.J., and Goodship, J.A. (2003). Mutations in two nonhomologous genes in a head-to-head configuration cause Ellis-van Creveld syndrome. Am. J. Hum. Genet. *72*, 728–732.
30. Valencia, M., Lapunzina, P., Lim, D., Zannolli, R., Bartholdi, D., Wollnik, B., Al-Ajlouni, O., Eid, S.S., Cox, H., Buoni, S., et al. (2009). Widening the mutation spectrum of EVC and EVC2: ectopic expression of Weyer variants in NIH 3T3 fibroblasts disrupts Hedgehog signaling. Hum. Mutat. *30*, 1667–1675.
31. Bachmann, V.A., Mayrhofer, J.E., Ilouz, R., Tschaikner, P., Raffeiner, P., Röck, R., Courcelles, M., Apelt, F., Lu, T.W., Baillie, G.S., et al. (2016). Gpr161 anchoring of PKA consolidates GPCR and cAMP signaling. Proc. Natl. Acad. Sci. USA *113*, 7786–7791.
32. Linglart, A., Menguy, C., Couvineau, A., Auzan, C., Gunes, Y., Cancel, M., Motte, E., Pinto, G., Chanson, P., Bougnères, P., et al. (2011). Recurrent PRKAR1A mutation in acrodysostosis with hormone resistance. N. Engl. J. Med. *364*, 2218–2226.
33. Lee, H., Graham, J.M., Jr., Rimoin, D.L., Lachman, R.S., Krejci, P., Tompson, S.W., Nelson, S.F., Krakow, D., and Cohn, D.H. (2012). Exome sequencing identifies PDE4D mutations in acrodysostosis. Am. J. Hum. Genet. *90*, 746–751.
34. Michot, C., Le Goff, C., Goldenberg, A., Abhyankar, A., Klein, C., Kinning, E., Guerrot, A.M., Flahaut, P., Duncombe, A., Baujat, G., et al. (2012). Exome sequencing identifies PDE4D mutations as another cause of acrodysostosis. Am. J. Hum. Genet. *90*, 740–745.
35. Kirschner, L.S., Carney, J.A., Pack, S.D., Taymans, S.E., Giatzakis, C., Cho, Y.S., Cho-Chung, Y.S., and Stratakis, C.A. (2000). Mutations of the gene encoding the protein kinase A type I-alpha regulatory subunit in patients with the Carney complex. Nat. Genet. *26*, 89–92.
36. Mateus, C., Palangié, A., Franck, N., Groussin, L., Bertagna, X., Avril, M.F., Bertherat, J., and Dupin, N. (2008). Heterogeneity of skin manifestations in patients with Carney complex. J. Am. Acad. Dermatol. *59*, 801–810.
37. Orellana, S.A., and McKnight, G.S. (1992). Mutations in the catalytic subunit of cAMP-dependent protein kinase result in unregulated biological activity. Proc. Natl. Acad. Sci. USA *89*, 4726–4730.
38. Cadd, G., and McKnight, G.S. (1989). Distinct patterns of cAMP-dependent protein kinase gene expression in mouse brain. Neuron *3*, 71–79.
39. Monies, D., Abouelhoda, M., Assoum, M., Moghrabi, N., Rafiullah, R., Almontashiri, N., Alowain, M., Alzaidan, H., Alsayed, M., Subhani, S., et al. (2019). Lessons Learned from Large-Scale, First-Tier Clinical Exome Sequencing in a Highly Consanguineous Population. Am. J. Hum. Genet. *104*, 1182–1201.
40. Sobreira, N., Schiettecatte, F., Valle, D., and Hamosh, A. (2015). GeneMatcher: a matching tool for connecting investigators with an interest in the same gene. Hum. Mutat. *36*, 928–930.